A Journal of the Gesellschaft Deutscher Chemiker

Angewandte International Edition

GDCh

Chemie

www.angewandte.org

Accepted Article

Title: Renal-clearable Macromolecular Reporter for Near-infrared Fluorescence Imaging of Bladder Cancer

Authors: Kanyi Pu, Jiaguo Huang, Yuyan Jiang, Jingchao Li, Shasha He, and Jingsheng Huang

To be cited as: *Angew. Chem. Int. Ed.* 10.1002/anie.201911859
Angew. Chem. 10.1002/ange.201911859

Link to VoR: http://dx.doi.org/10.1002/anie.201911859
http://dx.doi.org/10.1002/ange.201911859

WILEY-VCH

10.1002/anie.201911859

WILEY-VCH

RESEARCH ARTICLE

Molecularly Engineered Macrophage-Derived Exosomes with Inflammation Tropism and Intrinsic Biosynthesis for Atherosclerosis Treatment

Guanghao Wu[a], Qianru Zhao[a], Wanru Zhuang[a], Jingjing Ding[a], Chi Zhang[c], Haijun Gao[a], Dai-Wen Pang[b], Jinfeng Zhang[a], Kanyi Pu*[c], Hai-Yan Xie*[a]

Abstract: Atherosclerosis is a major contributor to cardiovascular diseases worldwide, and anti-inflammation is a promising strategy for atherosclerosis treatment. Despite the progress made with recent use of nanocarriers, development of effective atherosclerosis targeting and inflammation-alleviation strategy is still challenging. Here, we report the molecularly engineered M2 macrophage-derived exosomes (M2 Exo) with inflammation-tropism and anti-inflammatory capabilities for atherosclerosis imaging and therapy. These engineered M2 Exo are derived from M2 macrophages and further electroporated with an FDA-approved hexyl 5-aminolevulinate hydrochloride (HAL). After systematic administration, the engineered M2 Exo exhibit excellent inflammation-tropism and anti-inflammation effects *via* the surface-bonded chemokine receptors and released anti-inflammatory cytokines from the anti-inflammatory M2 macrophages. Moreover, the encapsulated HAL can undergo intrinsic biosynthesis and metabolism of heme to generate anti-inflammatory carbon monoxide and bilirubin, which further enhance the anti-inflammation effects and finally alleviate atherosclerosis. Meanwhile, the intermediate protoporphyrin IX (PpIX) of heme biosynthesis pathway permits the fluorescence imaging and tracking of atherosclerosis. These M2 Exo engineered with inherent inflammation tropism and intrinsic biosynthesis of anti-inflammatory molecules can open a new avenue towards the treatment of atherosclerosis.

Introduction

Atherosclerosis is a major contributor to cardiovascular diseases which is one of the leading causes of morbidity and mortality worldwide. Inflammation is not only the key indication of atherosclerosis but also drives the whole disease progression.[1] Therefore, anti-inflammation has been regarded as a promising strategy for atherosclerosis treatment.[2] Despite some remarkable successes, the existing clinical anti-atherosclerotic drugs are lack of specific targeting capability toward the inflammatory sites and usually show poor half-life, which not merely compromise their practical therapeutic efficacy but also result in numerous side effects, even lead to death. Fortunately, inflammation generally accompanies with leaky vasculature, thus nanoparticles can passively accumulate in the pathological areas. Various nanocarriers have been designed to load and deliver drugs to atherosclerotic sites with improved permeability and retention.[3] However, the nanoparticle-based drug-delivery systems still suffer from some inherent disadvantages, such as the immunogenicity and toxicity of the carrier itself, fast immune recognition and blood clearance, and poor biodistribution.[4] Consequently, developing more reliable and powerful approaches for the atherosclerosis treatment are highly desired but challenging.

Very recently, considerable progresses have been made in the field of exosomes which are secreted nanovesicles (30–150 nm) from various cell types, featuring with fascinating natural properties, including outstanding biocompatibility, low cytotoxicity, immunological inertness, specific targeting and long-term circulating capability, making them effective drug delivery vehicles.[5] Exosomes derived from tumor cells, immune cells and mesenchymal stem cells are successfully applied in encapsulating and delivering chemotherapeutic drugs, nucleic acid drugs, neurotransmitters and even nanoparticles for the treatment of different diseases, such as cancer and neurological diseases, but have been rarely used in cardiovascular diseases up to now.[6] Moreover, the specific accumulation of exosome-based drug delivery systems is still limited even though they are functionalized with targeting biomolecules, therefore, inevitably leading to some adverse effects. It is worth noting that besides the unique properties, exosomes enrich specific contents (*e.g.* RNA, DNA, proteins and small molecules) derived from the parental cells, thus grafting the native biological functions of original cells that may be directly used for disease treatment. For example, exosomes derived from different stem cells and cardiac progenitor cells can enhance the cardiac function following myocardial infarction owing to the abundant miRNA in the exosomes.[7] Interestingly, it has been recently reported that exosomes isolated from macrophages are of the intrinsic inflammation-tropism capability owing to the various chemokine receptors on their surface.[8] Moreover, M2 phenotype macrophages can secrete anti-inflammatory cytokines such as interleukin-10 (IL-10), interleukin-1Ra (IL-1Ra) and transforming growth factor (TGF-β), implying the potential anti-inflammation therapy effect of M2 macrophages-derived exosomes (M2 Exo).[9] However, both the inflammation targeting and anti-inflammation capabilities of M2 Exo have not been revealed yet to the best of our knowledge.

[a] G. Wu, Q. Zhao, W. Zhuang, J. Ding, H. Gao, Prof. J. Zhang, Prof. H. Xie
School of Life Science
Beijing Institute of Technology
No.5 South Zhong Guan Cun Street, Beijing, 100081 (China)
E-mail: hyanxie@bit.edu.cn
[b] D. Pang
Research Center for Analytical Sciences, College of Chemistry
Nankai University
No.94 Weijin Road, Nankai District, Tianjin, 300071 (China)
[c] C. Zhang, Prof. K. Pu
School of Chemical and Biomedical Engineering, Nanyang Technological University, Singapore, 637457, Singapore
E-mail: kypu@ntu.edu.sg

Supporting information and the ORCID identification number(s) for the author(s) of this article can be found under: https://doi.org/

10.1002/anie.201911859
WILEY-VCH

RESEARCH ARTICLE

Herein, we molecularly engineer the M2 Exo to endow them with inherent inflammation tropism and intrinsic biosynthesis functionality for effective targeting and potent treatment of atherosclerosis. The M2 Exo are collected from M2 macrophages are further electroporated with an FDA-approved hexyl 5-aminolevulinate hydrochloride (HAL) to obtain HAL-containing M2 exosomes (HAL@M2 Exo).[10] After systemic administration, the as-prepared HAL@M2 Exo can bind to the inflammatory endothelial cell in atherosclerosis sites *via* the chemokine receptors presented on M2 Exo surface, and subsequently undergo tethering, rolling, adhering and transmigrating across the endothelial cell layers, eventually accumulating in the atherosclerosis lesions.[11] Then, the uptake of HAL@M2 Exo by inflammatory cells leads to the release of endogenous anti-inflammatory cytokines and exogenous HAL. HAL initiates the subsequent biosynthesis and metabolism of heme to produce two extra anti-inflammatory compounds, carbon monoxide (CO) and bilirubin.[12] The anti-inflammatory cytokines together with CO and bilirubin significantly alleviate the inflammation-induced atherosclerosis *in vivo*. Meanwhile, the intermediate protoporphyrin IX (PpIX) of heme biosynthesis pathway can be further used for fluorescence imaging and tracking of atherosclerosis.[13] The smart engineered and self-biosynthesizable exosomes show great potential as a reliable candidate for atherosclerosis treatment.

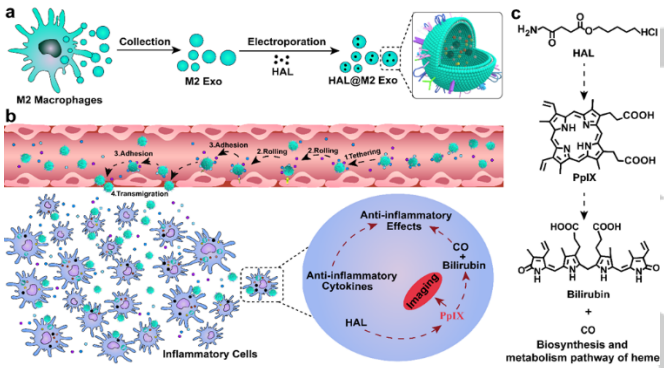

Figure 1. Scheme illustration of the anti-atherosclerosis treatment by using HAL@M2 Exo. a) The preparation of HAL@M2 Exo. b) The inflammation-tropism and anti-inflammation effect of HAL@M2 Exo. c) The simplified biosynthesis and metabolism pathway of heme induced by HAL.

Results and Discussion

Preparation and characterization of the HAL loading M2 Exo. The pristine macrophages (M0) were firstly polarized to M2 phenotype by culturing RAW264.7 cells with interleukin-4 (IL-4) (Figure S1). The corresponding M2 Exo collected by differential ultracentrifugation were well dispersed with cup-shaped nanostructure of approximate 180 nm in diameter (Figure 2a). They were rich in M2 biomarkers (CD206 and CD163) as characterized by different methods including flow cytometry, western blotting and confocal laser scanning microscopy (CLSM), in which CD63 is a representative exosome protein (Figure 2b-d). Afterwards, the hydrophilic HAL molecules were encapsulated into M2 Exo through electroporation. The successful HAL loading was confirmed by high-performance liquid chromatography (HPLC) analysis, and the loading capacity as well as encapsulation efficiency of HAL were determined to be 25.14 % and 19.34 %, respectively (Figure 2e and Figure S2). The average size and zeta potential of the as-prepared HAL@M2 Exo exhibited similar results as those of M2 Exo alone (Figure 2f), indicating that the surface properties of M2 Exo would not be changed greatly after drug loading. Furthermore, both M2 Exo and HAL@M2 Exo showed excellent colloidal stability in phosphate buffered saline (PBS) in a week (Figure 2g).

Generally, macrophages are defined as two phenotypes including pro-inflammatory M1 phenotype and anti-inflammatory M2 phenotype.[14] We then comparatively evaluated the secretion levels of anti-inflammatory cytokines (*e.g.*, IL-10, IL-1Ra and TGF-β) and pro-inflammatory cytokines (*e.g.*, interleukin-6 (IL-6), tumor necrosis factor (TNF-α) and metalloproteinase-10 (MMP-10)) in exosomes derived from pristine macrophages (M0 Exo), exosomes derived from M1-polarized macrophages (M1 Exo) (Figure S3), M2 Exo and HAL@M2 Exo. As presented in Figure 2h, both M2 Exo and HAL@M2 Exo showed much higher level of anti-inflammatory factors but much lower quantity of pro-inflammatory factors when compared with M0 Exo and M1 Exo, suggesting the potential anti-inflammatory responses of M2 Exo. For further verification, the inflammatory M1 cells were treated with M2 Exo or HAL@M2 Exo for 24 h, and then the phenotype transition of cells was evaluated by flow cytometry. We were glad to find that M2 Exo or HAL@M2 Exo treatment could significantly induce the reprogramming of inflammatory M1 cells as illustrated by the clearly increased expression of M2 biomarkers: CD206 and CD163; meanwhile the dramatically decrease of M1 biomarkers: CD80 and CD86, indicating the effective anti-inflammatory performance of M2 Exo and HAL@M2 Exo (Figure 2i).

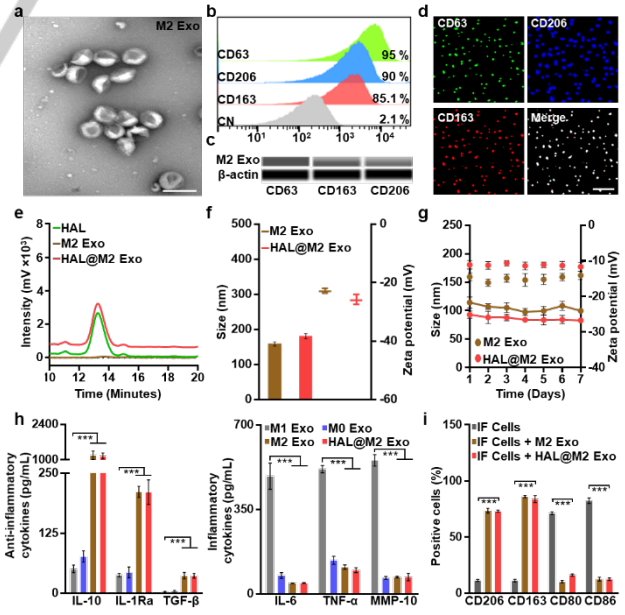

Figure 2. Characterization of M2 Exo. a) TEM image of M2 Exo. Scale bar: 200 nm. b, c) Flow cytometry and western blotting analysis of CD63, CD206 and CD163 expressed on M2 Exo. d)

10.1002/anie.201911859

Fluorescence colocalization of CD63, CD206 and CD163 on M2 Exo. Scale bar: 1μm. e) HPLC analysis of HAL in M2 Exo. f) Sizes and zeta potentials of M2 Exo and HAL@M2 Exo. g) The stability of M2 Exo and HAL@M2 Exo during 7 days incubation monitored according to the size and zeta potential in PBS. h) The content of anti-inflammatory and pro-inflammatory cytokines in different exosomes. i) Flow cytometry analysis of CD206, CD163, CD80 or CD86 positive inflammatory cells before and after different treatments. The results represent the mean ± standard deviation (n = 3).

Efficient biosynthesis and metabolism of heme induced by HAL in cells. It is reported that HAL can be enzymatically synthesized to the intermediate protoporphyrin IX (PpIX) in Figure 3a. In the downstream biosynthesis, the PpIX is converted into heme, which then efficiently converts into CO and bilirubin as the final catabolic metabolites in cells.[15] Firstly, to verify the formation of PpIX, characteristic red fluorescence of PpIX was visualized by CLSM. As shown in Figure 3b, both free HAL or HAL@M2 Exo treated inflammatory cells exhibited clearly bright red signals, whereas M2 Exo alone or PBS treated groups showed negligible fluorescence, indicating that diagnostic molecule PpIX could be successfully biosynthesized from HAL substrate in the cells. Notably, red signals of PpIX substantially increased in cells upon addition of heme oxygenase-1 (HO-1) inhibitor, which were attributed to the blocking of downstream pathway and thus the enhanced accumulation of PpIX. To further confirm the successful generation of the final metabolites, CO was detected trough CLSM by using an allyl chloroformate functionalized fluorescein (FL-CO-1) as the CO sensor and bilirubin was detected by ELISA assay.[16] As expected, HAL-containing groups showed the obvious CO and bilirubin production (Figure 3c and d). In contrast, these two metabolites were hard to find in the absence of HAL or in the presence of HO-1 inhibitor because lacking of essential substrate or requisite enzyme. Interestingly, it was also found that more metabolic products could be formed in HAL@M2 Exo treated cells compared with free HAL treated group, probably because that the high hydrophilicity of HAL molecules would reduce its transmembrane transport while M2 Exo could improve the uptake through endocytosis and membrane fusion. To further support the above results, we detected the expression levels of three key catalytic enzymes including uroporphyrinogen decarboxylase (UROD) and protoporphyrinogen oxidase (PPOX) that related to the PpIX biosynthesis as well as HO-1 that associated with the bilirubin generation. It could be found that all the three enzyme levels were remarkably up-regulated in HAL or HAL@M2 Exo treated inflammatory cells (Figure 3e-g), which were well in accordance with the above results. All together, these results strongly suggested that exogenous HAL molecules could prominently augment the enzyme-catalyzed biosynthesis and metabolism of heme, synchronously generating the corresponding functional intermediate and metabolites.

Excellent Inflammation-tropism capability of HAL@M2 Exo. To evaluate the potential inflammation-tropism capability of the as-prepared HAL@M2 Exo and clarify its relevant mechanisms, we conducted a series of *in vitro* experiments to investigate the presence of representative adhesion molecules and chemokine

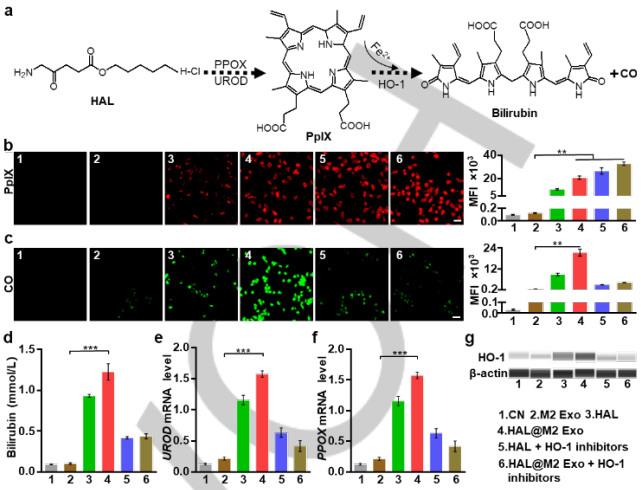

Figure 3. The biosynthesis and metabolism of heme induced by HAL in inflammatory cells. a) Simplified pathway. b, c) Fluorescence imaging and corresponding mean fluorescence intensity (MFI) statistics of PpIX or CO in cells after different treatments. Scale bar: 5 μm. d) ELISA assays for bilirubin in cells after different treatments. e, f) RT-PCR analysis for mRNA level of UROD or PPOX in cells after different treatments. g) Western blotting analysis of HO-1 in cells after different treatments. The results represent the mean ± standard deviation (n = 3).

receptors associated to M2 Exo recruitment (Figure 4a). Firstly, the CLSM imaging, western blotting and flow cytometry analyses of both M2 Exo and HAL@M2 Exo verified the presence of three chemokine receptors including CC chemokine receptor type 2 (CCR2), CXC chemokine receptor 2 (CXCR2) and CXC chemokine ligand 2 (CXCL2) (Figure 4b, c and Figure S4), which would respond to the inflammatory stimuli thus lead to the slowing down and recruitment of M2 Exo based nanovehicles at inflammatory sites. Then, the expression of adhesion molecules including E-selectin, vascular cell adhesion molecule 1 (VCAM1) and endothelial intercellular adhesion molecule 1 (ICAM1) on inflammatory endothelial cells as well as their corresponding chemokine receptors including CD44, monocyte very late antigen 4 (VLA4), and monocyte lymphocyte function-associated antigen 1 (LFA1) presented on M2 Exo membranes were respectively examined by flow cytometry and western blotting. As depicted in Figure 4d-g, the adhesion molecules were up-regulated on activated human umbilical vein endothelial cells (HUVECs) compared with the normal HUVECs; meanwhile, both M2 Exo and HAL@M2 Exo showed high levels of the three receptors, suggesting the strong molecular recognition between the HAL@M2 Exo and activated HUVECs. Therefore, the initially recruited M2 Exo or HAL@M2 Exo would firmly adhere to the activated inflammatory endothelial cells *via* the E-selectin-CD44, VCAM1-VLA4, and ICAM1-LFA1 interactions, which would further facilitate their following transmigration. Moreover, the platelet endothelial cell adhesion molecule (PECAM), one of the endothelial transmembrane proteins playing important roles in regulating transmigration,[17] was concurrently highly expressed on M2 Exo based nanovehicles and activated HUVECs (Figure 4d-g), which would ultimately lead to the superior transmigration

10.1002/anie.201911859

RESEARCH ARTICLE

and accumulation of M2 Exo based nanovehicles at inflammation sites.

To further confirm the transmigration capability and uptake efficiency of the HAL@M2 Exo, *in vitro* Transwell assays were subsequently carried out as illustrated in Figure 4g. A monolayer of activated HUVECs and inflammatory cells were respectively incubated on the top chamber and bottom chamber for 24 h. Then, four groups including (1): M2 Exo, (2): M2 Exo + LPS, (3): HAL@M2 Exo, and (4): HAL@M2 Exo + LPS were individually added to the upper chamber of the Transwell models. In LPS induced inflammatory microenvironment, both M2 Exo and HAL@M2 Exo exhibited dramatically higher efficiency of transmigrating into basolateral chamber supernatant and enhanced accumulation in inflammatory cells. In contrast, much lower transmigration and uptake efficiency of both M2 Exo or HAL@M2 Exo without LPS stimulation. All these results together proved that HAL@M2 Exo were of excellent inflammation-tropism capability owing to the intrinsic inflammatory affinities originating from polarized M2 macrophages, which would be beneficial for the following *in vitro* and *in vivo* anti-inflammation treatment.

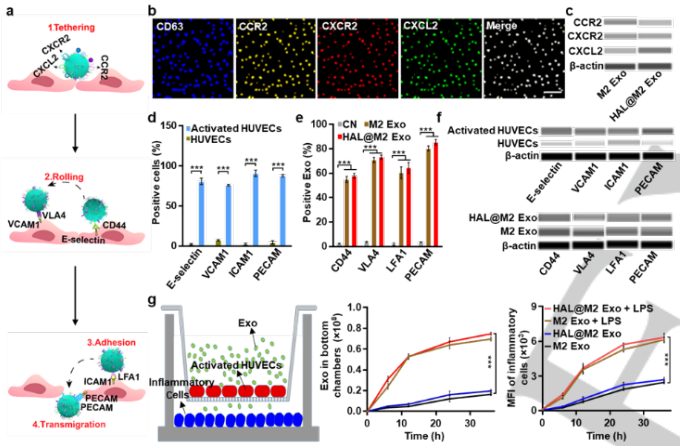

Figure 4. Inflammation-tropism of M2 Exo. a) Schematic model of Exo adhesion cascade in the inflammatory sites. b) Fluorescence imaging of chemokine receptors CCR2, CXCR2 and CXCL2 on M2 Exo by using CD63 as the marker of exosomes. Scale bar: 1μm. c) Western blotting analysis of chemokine receptors CCR2, CXCR2 and CXCL2 on M2 Exo or HAL@M2 Exo. d) Flow cytometry analysis of cell-adhesion molecules E-selectin, VCAM1, ICAM1 or PECAM positive HUVECs and activated HUVECs. e) Flow cytometry analysis of receptors CD44, VLA4, LFA1 or PECAM positive M2 Exo and HAL@M2 Exo. f) Western blotting analysis of corresponding adhesion molecules and receptors in d, e. g) The established Transwell model and time-dependent quantification of M2 Exo or HAL@M2 Exo in the supernatant or inflammatory cells of bottom chamber.The results represent the mean ± standard deviation (n = 3).

Enhanced *In vitro* anti-inflammation effect of HAL@M2 Exo. After validating the favorable tropism capability of HAL@M2 Exo, we next comparatively examined the anti-inflammation effect of HAL, M2 Exo and HAL@M2 Exo in common inflammatory cells stimulated by LPS or typical foam cells simultaneously induced by oxidized low-density lipoprotein (oxLDL) and LPS. Firstly, the status of oxidative stress including generation of reactive oxygen species (ROS) and inducible nitric oxide synthase (iNOS) as well as expression of typical pro-inflammatory cytokines including MMP-10, IL-6, TNF-α and interleukine-1β (IL-1β) were evaluated in common inflammatory cells. As depicted in Figure 5a-c, benefiting from the satisfactory anti-inflammation effect of HAL and M2 Exo, both oxidative species and inflammatory cytokines were obviously reduced in free HAL or M2 Exo treated groups compared with the PBS control group (CN). Importantly, these decreases were further significantly enhanced in the cells treated with HAL@M2 Exo.

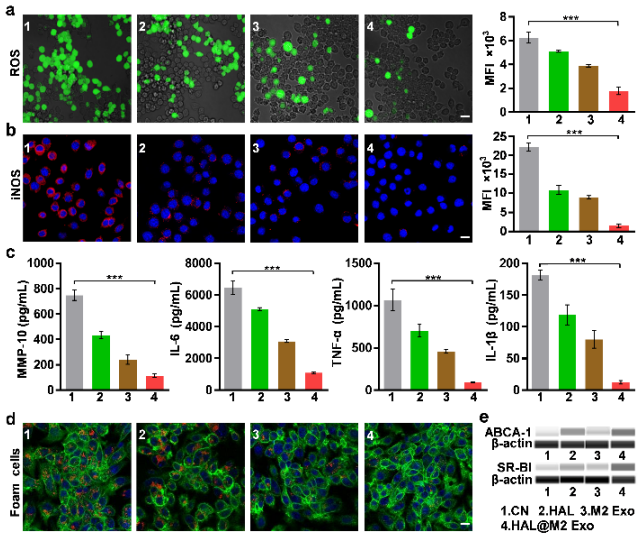

Figure 5. Anti-inflammation and promoting cholesterol efflux effects of HAL@M2 Exo. a) Fluorescence imaging of ROS (Green: DCFH-DA labeled ROS) in inflammatory cells after different treatments. Scale bar: 20 μm. b) Immunofluorescence analysis of iNOS in inflammatory cells (Red: iNOS; Blue: cell nuclei). Scale bar: 20 μm. c) ELISA assays of typical pro-inflammatory cytokines in inflammatory cells after different treatments. d) Fluorescence imaging of oxLDL in foam cells after different treatments (Red: DiI-labeled oxLDL; Blue: cell nuclei; Green: cell membrane). Scale bar: 20 μm. e) Western blotting analyses of ABCA-1 and SR-BI in the foam cells after different treatments. The results represent the mean ± standard deviation (n = 3).

Subsequently, we investigated the anti-inflammation effect of HAL@M2 Exo on foam cells which are crucial underpinnings to early atherosclerosis establishment.[18] Notably, treatment of the foam cells with free HAL, M2 Exo or HAL@M2 Exo could greatly decrease the intracellular oxLDL content (Figure 5d and Figure S5), which is a fundamental element involved in the progression of foam cells. In addition, the expression levels of ATP-binding cassette subfamily-A transporters-1 (ABCA-1) and scavenger receptor class B type I (SR-BI) on foam cells after treatment were also greatly up-regulated compared with the PBS control group (Figure 5e), revealing that either HAL or M2 Exo containing samples could facilitate the cholesterol efflux in foam cells because these two receptors are responsible for the reverse cholesterol transport (RCT) pathway. Notably, both the levels of

10.1002/anie.201911859

ABCA-1 and SR-BI in HAL@M2 Exo treated group were clearly higher than the other groups. Such RCT upregulation would be further in favor of the ultimate anti-atherosclerotic outcome of HAL@M2 Exo. Collectively, all these data implicated that the combination of HAL and M2 Exo could effectively enhance the *in vitro* anti-inflammation capability and HAL@M2 Exo is potentially applied to the following *in vivo* therapy.

Superior *in vivo* anti-inflammation therapy in acute peritonitis. Encouraged by the great inflammation-tropism and inflammation-alleviation capabilities of HAL@M2 Exo *in vitro*, we next investigated their *in vivo* performance by using an acute peritonitis mouse model. The BALB/c mice were firstly intraperitoneally injected with sterile zymosan solution (0.5 mL, 2 mg/mL).[19] After 12 h, different formulations including free HAL, M2 Exo and HAL@M2 Exo were intravenously injected into the mice respectively, and PBS was used as the control group. Time-dependent *in vivo* accumulations of HAL or HAL@M2 Exo were tracked by using the intrinsic fluorescence of HAL-converted PpIX. It was observed that most HAL@M2 Exo could target and accumulate in inflammatory abdominal cavity (indicated by the red circles) while free HAL molecules were mainly located in other sites, especially in liver (Figure 6a and Figure S6), demonstrating the as-designed HAL@M2 Exo can effectively target to inflammation sites and generate diagnostic signals *in situ* for *in vivo* imaging.

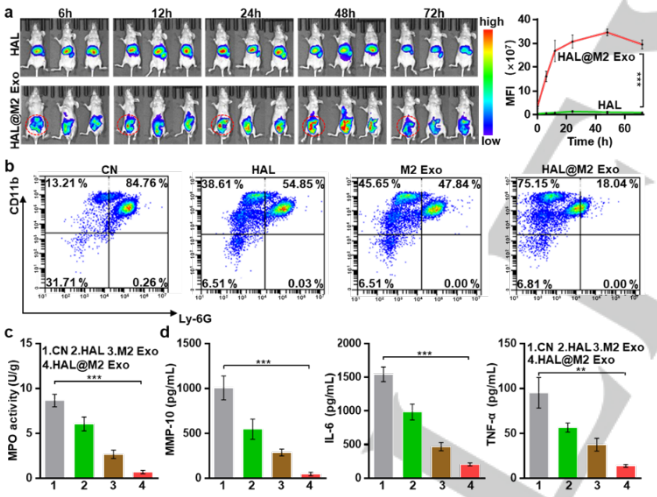

Figure 6. *In vivo* imaging and treatment of acute peritonitis using HAL@M2 Exo. a) Fluorescence imaging of mice with acute peritonitis at different time intervals after treatment with HAL or HAL@M2 Exo. b, c) Flow cytometric analysis of neutrophils and MPO activity in neutrophils in acute peritoneal exudates 24 h after different treatments. d) ELISA assay of the expression levels of typical pro-inflammatory cytokines in acute peritoneal exudates 24 h after different treatments. The results represent the mean ± standard deviation (n = 6).

As is well-documented that dysregulated neutrophils play considerable roles in inducing or even aggravating acute inflammation-related diseases by releasing proteases and ROS to the impaired tissues or organs.[20] Hence, to evaluate the therapeutic effect of HAL@M2 Exo on this acute model, total number of neutrophils in peritoneal exudates as well as the enzymatic activity of myeloperoxidase (MPO) which is a typical marker for neutrophils were determined 24 h after treatments. As shown in Figure 6b and c, a large number of neutrophils infiltrated and sequestrated in abdominal cavity and high MPO activity exhibited in the control group. By contrast, administration of HAL or M2 Exo based formulations could effectively diminish the retention of infiltrated neutrophils in abdominal cavities, meanwhile decrease the MPO activity. Particularly, the HAL@M2 Exo treated group displayed the lowest proportion of neutrophils in peritoneal exudates, reflecting that HAL@M2 Exo could significantly ameliorate acute peritonitis. Besides, the expression levels of pro-inflammatory cytokines including MMP-10, IL-6, TNF-α and IL-1β were correspondingly downregulated (Figure 6d and Figure S7), further confirming that HAL@M2 Exo can substantially alleviate inflammation *in vivo*.

Efficient *In vivo* treatment of early atherosclerosis. Finally, we were in the position to evaluate the therapeutic effect of HAL@M2 Exo on atherosclerosis. Firstly, an early atherosclerosis mouse model was established by fed the ApoE deficient (ApoE$^{-/-}$) mice (male, 6-8 weeks) with cholesterol-rich diet for 12 weeks,[21] and then randomly divided into four groups and intravenously injected with PBS, HAL, M2 Exo or HAL@M2 Exo (5.5 mg/kg HAL-equivalent and 9 mg/kg M2-equivalent), respectively (Figure 7a). After 24 h, the aortas and major organs including liver, spleen, lung and kidney were excised from the mice treated with free HAL or HAL@M2 Exo. It was found that the fluorescence originating from endogenously biosynthesized PpIX in aortas of mice injected with HAL@M2 Exo was much higher than that in free HAL treated mice. More encouragingly, the HAL@M2 Exo treated group exhibited the highest PpIX fluorescence signal in aortas among all collected major organs (Figure 7b and Figure S8), again demonstrating the specific inflammation-tropism of HAL@M2 Exo, which was of great importance to boost its ultimate therapeutic performance.

After 5 weeks treatments, the mice were all sacrificed. Then their entire aortas as well as aortic valves were excised for Oil Red O (ORO) staining which was applied for detecting lipid deposits in atherosclerotic plaques (Figure 7c and d). Comparatively, treatment with HAL@M2 Exo performed the optimal anti-atherosclerotic effect where 75.2 % reduction of inflammation-induced aortas lesion area as well as 73.9 % reduction of aortic valves lesions were achieved in comparison with the PBS control group. Then histological examination on aortic valves stained with hematoxylin and eosin (H&E) was further carried out to directly assess the anti-inflammatory outcome. As expected, necrosis areas in the aortic valves were obviously diminished after treatment with HAL@M2 Exo, which was also consistent with the corresponding quantitative analyses (Figure 7e). After that, we accordingly evaluated the expression levels of ABCA-1 and SR-BI receptors in aortas by western blotting. In contrast to the control group, these two RCT-pathway-modulated protein receptors were greatly up-regulated in other three groups due to the improved cholesterol-efflux capability of HAL or M2 Exo based formulations (Figure 7f), which agreed well with the above-mentioned *in vitro* results. These results together revealed that HAL@M2 Exo could

effectively relieve chronic inflammation-induced atherosclerosis *in vivo*. Moreover, treatment with HAL@M2 Exo resulted in few abnormalities in the organ histology and blood biochemical markers (Figure S9), suggesting its good biocompatibility and safe use.

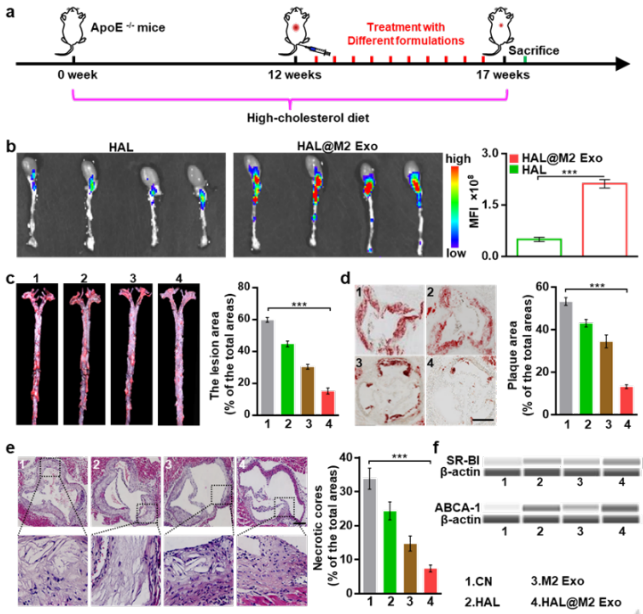

Figure 7. Treatment of early atherosclerotic plaques with HAL@M2 Exo. a) Schematic diagram of the treatment protocol. b) Fluorescence imaging of the aortas excised from mice. c) Photographs of the excised aortas stained by ORO and the corresponding quantitative analyses of plaque areas. d) Cryosection photographs of the aortic valves stained by ORO and the corresponding quantitative analyses of plaque areas. Scale bar: 300 μm. e) H&E staining images and the necrosis area statistics of aortic valves after different treatments. Scale bar: 200 μm. f) Western blotting analyses of ABCA-1 and SR-BI. The results represent the mean ± standard deviation (n = 6).

Conclusion

In this study, we have pioneered the deveolpment of HAL-engineered M2 macrophage-derived exosomes for effective treatment of atherosclerosis. The HAL@M2 Exo can not only exert the superiority of anti-inflammatory M2 macrophages for simultaneously targeting and alleviating inflammation in the atherosclerosis lesions by surface-bonded chemokine receptors and secreted anti-inflammatory cytokines, but also utilize the FDA-approved natural precursor HAL for heme biosynthesis *via* a series of enzyme-catalyzed reactions to generate extra anti-inflammatory CO and bilirubin with boosting therapeutic effects. Moreover, the red-fluorescent intermediate PpIX during HAL-mediated heme biosynthesis processes exhibited fluorescence imaging and tracking of atherosclerosis. Both *in vitro* and *in vivo* experimental results demonstrated the remarkable inflammation-tropism and inflammation-alleviation effects of the as-prepared HAL@M2 Exo. These HAL-engineered M2 macrophage-derived exosomes would be promising for the treatment of atherosclerosis and even many inflammation-associated diseases in future.

Experimental Section

See the Supporting Information for experimental section.

Acknowledgements

We thank Biological & Medical Engineering Core Facilities (Beijing Institute of Technology) for providing advanced equipment. This work was supported by the National Natural Science Foundation of China (No. 91859123, and 21874011), National Science and Technology Major Project (No. 2018ZX 10301405-001), and China Postdoctoral Science Foundation (No. 2018M630076).

Conflict of interest

The authors declare no conflict of interest

Keywords: exosomes • inflammation • membrane proteins • biosynthesis

[1] C. Weber, H. Noels, *Nat Med* **2011**, *17*, 1410–1422.
[2] a) M. Bäck, G. K. Hansson, *Nat Rev Cardiol* **2015**, *12*, 199–211; b) I. Tabas, C. K. Glass, *Science* **2013**, *316*, 166–172; c) H. Zhu, Y. Fang, Q. Miao, X. Qi, D. Ding, P. Chen, K. Pu, *ACS Nano* **2017**, *11*, 8998–9009..
[3] a) J. H. Park, D. Dehaini, J. Zhou, M. Holay, R. H. Fang, L. Zhang, *Nanoscale Horiz.* **2019**, *10*.1039.C9NH00291J; b) X. Wei, M. Ying, D. Dehaini, Y. Su, A. V. Kroll, J. Zhou, W. Gao, R. H. Fang, S. Chien, L. Zhang, *ACS Nano* **2018**, *12*, 109–116; c) M. E. Lobatto, V. Fuster, Z. A. Fayad, W. J. M. Mulder, *Nat Rev Drug Discov* **2011**, *10*, 835–852; d) J. Li, K. Pu, *Chem. Soc. Rev.* **2019**, *48*, 38-71.
[4] a) J. Zhang, Y. Zu, C. S. Dhanasekara, J. Li, D. Wu, Z. Fan, S. Wang, *WIREs Nanomed Nanobiotechnol* **2017**, *9*, e1412; b) C. K. W. Chan, L. Zhang, C. K. Cheng, H. Yang, Y. Huang, X. Y. Tian, C. H. J. Choi, *Small* **2018**, *14*, 1702793; c) W. J. M. Mulder, F. A. Jaffer, Z. A. Fayad, M. Nahrendorf, *Science Translational Medicine* **2014**, *6*, 239sr1-239sr1.
[5] a) F. Fernandez-Trillo, L. M. Grover, A. Stephenson-Brown, P. Harrison, P. M. Mendes, *Angew. Chem. Int. Ed.* **2017**, *56*, 3142–3160; b) Y. Jiang, M. Shi, Y. Liu, S. Wan, C. Cui, L. Zhang, W. Tan, *Angew. Chem. Int. Ed.* **2017**, *56*, 11916–11920; c) K. Mori, M. Hirase, T. Morishige, E. Takano, H. Sunayama, Y. Kitayama, S. Inubushi, R. Sasaki, M. Yashiro, T. Takeuchi, *Angew. Chem. Int. Ed.* **2019**, *58*, 1612–1615.
[6] a) P. H. L. Tran, D. Xiang, T. T. D. Tran, W. Yin, Y. Zhang, L. Kong, K. Chen, M. Sun, Y. Li, Y. Hou, et al., *Adv. Mater.* **2019**, 1904040; b) Y. Lyu, D. Cui, J. Huang, W. Fan, Y. Miao, K. Pu, *Angew. Chem. Int. Ed.* **2019**, *58*, 4983–4987; c) X. Gao, S. Li, F. Ding, H. Fan, L. Shi, L. Zhu, J. Li, J. Feng, X. Zhu, C. Zhang, *Angew. Chem. Int. Ed.* **2019**, *58*, 8719–8723.
[7] M. Adamiak, S. Sahoo, *Molecular Therapy* **2018**, *26*, 1635
[8] a) H. Kim, S. Y. Wang, G. Kwak, Y. Yang, I. C. Kwon, S. H. Kim, *Adv. Sci.* **2019**, 1900513; b) Y. W. Choo, M. Kang, H. Y. Kim, J. Han, S. Kang, J.-R. Lee, G.-J. Jeong, S. P. Kwon, S. Y. Song, S. Go, et al., *ACS Nano* **2018**, *12*, 8977–8993;

c) Q. Hu, C. Qian, W. Sun, J. Wang, Z. Chen, H. N. Bomba, H. Xin, Q. Shen, Z. Gu, *Adv. Mater.* **2016**, *28*, 9573–9580; d) Q. Zhang, D. Dehaini, Y. Zhang, J. Zhou, X. Chen, L. Zhang, R. H. Fang, W. Gao, L. Zhang, *Nature Nanotech* **2018**, *13*, 1182–1190; e) S. Thamphiwatana, P. Angsantikul, T. Escajadillo, Q. Zhang, J. Olson, B. T. Luk, S. Zhang, R. H. Fang, W. Gao, V. Nizet, et al., *Proc Natl Acad Sci USA* **2017**, *114*, 11488–11493;

[9] a) T. M. Raimondo, D. J. Mooney, *Proc Natl Acad Sci USA* **2018**, *115*, 10648–10653; b) J. Kim, H. Y. Kim, S. Y. Song, S. Go, H. S. Sohn, S. Baik, M. Soh, K. Kim, D. Kim, H.-C. Kim, et al., *ACS Nano* **2019**, *13*, 3206–3217; c) P. J. Murray, J. E. Allen, S. K. Biswas, E. A. Fisher, D. W. Gilroy, S. Goerdt, S. Gordon, J. A. Hamilton, L. B. Ivashkiv, T. Lawrence, et al., *Immunity* **2014**, *41*, 339–340; d) A. Aalipour, H.-Y. Chuang, S. Murty, A. L. D'Souza, S. Park, G. S. Gulati, C. B. Patel, C. Beinat, F. Simonetta, I. Martinić, et al., *Nat Biotechnol* **2019**, *37*, 531–539.

[10] a) E. L. P. Larsen, L. L. Randeberg, O. A. Gederaas, C.-J. Arum, A. Hjelde, C.-M. Zhao, D. Chen, H. E. Krokan, L. O. Svaasand, *J. Biomed. Opt.* **2008**, *13*, 044031; b) L. P. H. Yang, *Mol Diagn Ther* **2014**, *18*, 105–116.

[11] Y. Bi, J. Chen, F. Hu, J. Liu, M. Li, L. Zhao, *Neural Plasticity* **2019**, *2019*, 1–21.

[12] a) H. J. Kim, M.-Y. Jeong, T. J. Parnell, M. Babst, J. D. Phillips, D. R. Winge, *J. Biol. Chem.* **2016**, *291*, 17417–17426; b) D.-W. Zheng, J.-X. Fan, X.-H. Liu, X. Dong, P. Pan, L. Xu, X.-Z. Zhang, *Adv. Mater.* **2018**, *30*, 1801622; c) Y. Lee, H. Kim, S. Kang, J. Lee, J. Park, S. Jon, *Angew. Chem. Int. Ed.* **2016**, *55*, 7460–7463; c) R. Stocker, Y. Yamamoto, A. McDonagh, A. Glazer, B. Ames, *Science* **1987**,*235*, 1043–1046; d) S.-B. Wang, C. Zhang, Z.-X. Chen, J.-J. Ye, S.-Y. Peng, L. Rong, C.-J. Liu, X.-Z. Zhang, *ACS Nano* **2019**, *13*, 5523–5532.

[13] A.-N. Zhang, W. Wu, C. Zhang, Q.-Y. Wang, Z.-N. Zhuang, H. Cheng, X.-Z. Zhang, *J. Mater. Chem. B* **2019**, *7*, 1087–1095.

[14] a) P. M.-K. Tang, D. J. Nikolic-Paterson, H.-Y. Lan, *Nat Rev Nephrol* **2019**, *15*, 144–158; b) J. Li, H. Duan, K. Pu, *Adv. Mater.* **2019**, *31*, 1901607.

[15] a) M. Fujino, Y. Nishio, H. Ito, T. Tanaka, X.-K. Li, *International Immunopharmacology* **2016**, *37*, 71–78; b) M. Wachowska, A. Muchowicz, M. Firczuk, M. Gabrysiak, M. Winiarska, M. Wańczyk, K. Bojarczuk, J. Golab, *Molecules* **2011**, *16*, 4140–4164.

[16] a) D.-W. Zheng, B. Li, C.-X. Li, L. Xu, J.-X. Fan, Q. Lei, X.-Z. Zhang, *Adv. Mater.* **2017**, *29*, 1703822; b) W. Feng, D. Liu, S. Feng, G. Feng, *Anal. Chem.* **2016**, *88*, 10648–10653.

[17] a) E. P. C. van der Vorst, Y. Döring, C. Weber, *J Mol Med* **2015**, *93*, 963–971; b) D. Tousoulis, C. Antoniades, C. Stefanadis, *Heart* **2007**, *93*, 1001–1007; c) M. R. Williams, V. Azcutia, G. Newton, P. Alcaide, F. W. Luscinskas, *Trends in Immunology* **2011**, *32*, 461–469; d) Kolaczkowska, P. Kubes, *Nat Rev Immunol* **2013**, *13*, 159–175.

[18] G. Chinetti-Gbaguidi, S. Colin, B. Staels, *Nat Rev Cardiol* **2015**, *12*, 10–17.

[19] a) J. M. Schwab, N. Chiang, M. Arita, C. N. Serhan, *Nature* **2007**, *447*, 869–874; b) X. Xu, H. An, D. Zhang, H. Tao, Y. Dou, X. Li, J. Huang, J. Zhang, *Sci. Adv.* **2019**, *5*, 2953.

[20] a) M. Bäck, A. Yurdagul, I. Tabas, K. Öörni, P. T. Kovanen, *Nat Rev Cardiol* **2019**, *16*, 389–406; b) H. Zhao, Z. Zeng, L. Liu, J. Chen, H. Zhou, L. Huang, J. Huang, H. Xu, Y. Xu, Z. Chen, et al., *Nanoscale* **2018**, *10*, 6981–6991; c) Y. Lyu, J. Zeng, Y. Jiang, X. Zhen, T. Wang, S. Qiu, X. Lou, M. Gao, K. Pu, *ACS Nano* **2018**, *12*, 1801–1810.

[21] S. C. Whitman, *Clin Biochem Rev* **2004**, *25*, 81–93.

10.1002/anie.201911859

WILEY-VCH

Entry for the Table of Contents (Please choose one layout)

Layout 2:

RESEARCH ARTICLE

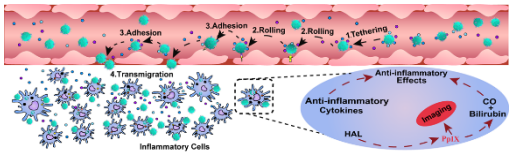

M2 macrophage-derived exosomes molecularly engineered with HAL can actively target and transmigrate to atherosclerotic lesions, wherein the biosynthesis and metabolism of heme induced by HAL produced CO and bilirubin. Together with anti-inflammatory cytokines in exosomes, the atherosclerosis is significantly alleviated. Meanwhile, the intermediate PpIX can be used for imaging and tracking of atherosclerosis.

Guanghao Wu, Qianru Zhao, Wanru Zhuang, Jingjing Ding, Chi Zhang, Haijun Gao, Dai-Wen Pang, Jinfeng Zhang, Kanyi Pu, Hai-Yan Xie**

Page No. – Page No.

Molecularly Engineered Macrophage-Derived Exosomes with Inflammation Tropism and Intrinsic Biosynthesis for Atherosclerosis Treatment